Low-frequency wake instability of an axisymmetric bluff body in pitch

Gentile, Valeria; Schrijer, Ferdinand; van Oudheusden, Bas; Scarano, Fulvio

Publication date
2016

Document Version
Accepted author manuscript

Published in
Proceeedings of the 18th International Symposium on the Application of Laser and Imaging Techniques to Fluid Mechanics

Low-frequency wake instability of an axisymmetric bluff body in pitch

V. Gentile[1,*], F. F. J. Schrijer[1], B. van Oudheusden[1], F. Scarano[1]
Department of Aerodynamics, Delft University of Technology, The Netherlands
* Correspondent author: v.gentile@tudelft.nl

Keywords: Turbulent axisymmetric wake, Azimuthal meandering, Stereoscopic PIV

ABSTRACT

The backflow instability in the wake past a cylindrical blunt-based body in pitch is investigated at a Reynolds number $Re_D = 6.7 \cdot 10^4$ based on the cylinder diameter. Time-resolved stereoscopic particle image velocimetry measurements have been performed in a cross-flow plane located $0.3\,D$ downstream of the model base. An increasing displacement of the backflow region from the body centerline with increasing pitch angles is observed in the long-time average of the velocity field, with the emergence of a preferred orientation of the wake. The time history of the backflow centroid position shows a progressive reduction of both amplitude and time scales of the fluctuations, reflecting the transition from large-scale azimuthal meandering to a more stable confinement at an off-center position. Proper Orthogonal Decomposition of the velocity fluctuations reveals a reduction by approximately 80% in the contribution of the first two modes for angles increasing up to 1°, accompanied by a distortion of the dipolar distribution typically associated with backflow meandering, for misalignments from 0.3° and higher. The frequency spectra of the POD time-coefficients display a very-low-frequency peak near $St_D \sim 10^{-3}$ only within 0.1° deviations from axisymmetric inflow conditions, thus endorsing the hypothesis that the long-term backflow instability only survives within small deviations from axisymmetric inflow conditions.

1. Introduction

Turbulent wake flows past bluff objects occur in many engineering applications and the large-scale wake instability developing in such flows at $Re > 10^2$ has been subject of numerous investigations[1]. Studies conducted on axisymmetric bodies such as disks[2] and spheres[3] have shown that this instability gives rise to an unsteady vortex-shedding mode with azimuthal wave number $m = 1$ at a non-dimensional frequency $St = 0.2$. Blunt-based bodies of interest to the automotive and space transportation industry exhibit this kind of unsteadiness with significant impact on the unsteady aerodynamic loads on the back of the body. A secondary instability linked with the vortex shedding and which has been more recently[4,5] discussed, entails the slow reorientation of the shedding plane, and consequently

of the recirculation bubble in the near-wake region, at non-dimensional frequencies in the order of $St = 10^{-3}$. The latter backflow meandering motion is identified as a very-low frequency contribution to the anti-symmetric mode $m = 1$, which is especially substantial near the base of the body[4,6]. As a consequence, notwithstanding the asymmetry of the instantaneous wake flow topology, statistical axisymmetry is achieved upon long-term averaging. This instability is currently regarded as the origin of the sensitivity of turbulent axisymmetric wake flows towards external perturbations[8,9] and poses important constraints on the required observation-time for achieving a proper statistical description, in both experimental and numerical investigations on such flows.

As this global mode reflects a number of equally probable asymmetrical wake topologies, the resulting statistical axisymmetry appears intrinsically related to the existence of symmetric inflow boundary conditions, which is not often the case for industrial configurations such as space launchers or submarines. The mean flow topology and turbulent statistics of an idealized submarine geometry in pitch and in yaw have been recently discussed by Ashok et al.[10,11], whereas in the case of ogive-cylinders the influence of external perturbations on the anti-symmetric global mode have been mainly investigated with respect to flow control approaches[9,12].

The aim of the present study is to characterize how this very-low-frequency backflow meandering evolves under conditions of angular misalignment of the body relative to the incoming flow. For this purpose stereoscopic particle image velocimetry (PIV) measurements are conducted in the near-wake of a cylindrical blunt-based body in non-zero pitch conditions, at $Re_D = 6.7 \cdot 10^4$, based on the model diameter. The measurements are conducted in a cross-flow plane located 0.3 D downstream of the trailing edge of the model. The long-time-averaged velocity fields are examined to evaluate the effects of the misalignment on the mean-flow topology, while the impact on the magnitude and characteristic time-scales of the backflow instability is assessed based on time-history of the backflow centroid position and snapshot proper orthogonal decomposition[13] (POD) of the velocity fluctuations.

2. Experimental setup

The experiments were conducted in an open-exit low-speed wind tunnel (W-Tunnel) of the Aerodynamics Laboratories of Delft University of Technology. The free stream velocity was $U_\infty = 20\ \mathrm{m/s}$ yielding a Reynolds number $Re_D = 6.7 \cdot 10^4$, based on the model diameter. The model consists of a cylindrical body with an ogive nose section (Fig. 1). Boundary layer

transition was enforced by means of a 10 mm wide roughness strip applied at the junction between nose and main body. A dedicated support allowed variations of the angle between the model symmetry axis and the incoming flow to be controlled with a precision of 0.03°. The pitch range investigated was between 0° and 1°.

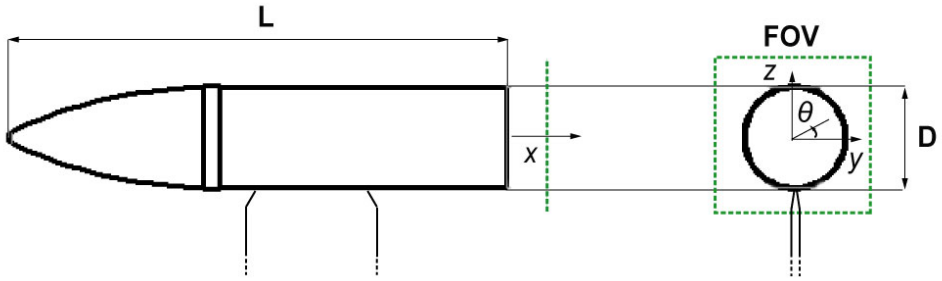

Fig. 1 Side and back view of the wind-tunnel model with coordinate system and measurement field of view (FOV).

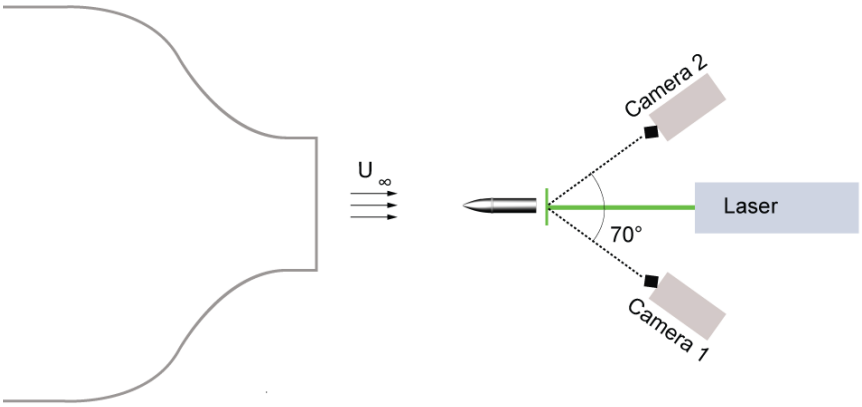

Fig. 2 Schematic top view of experimental setup with illumination and imaging configuration.

Stereoscopic particle image velocimetry (PIV) measurements were performed in a plane perpendicular to the symmetry axis of the model located at $x/D = 0.3$. The recordings were performed with two Photron *FastCAM* SA1.1 CMOS cameras (1024 x 1024 pixels, 5400 fps, 20 μm pixel) with an angle of 70° between the lines of sight (Fig. 2). The field of view (FOV) measured approximately 75 x 75 mm^2 (i.e. 1.5 D x 1.5 D) and was centered on the model axis. The optical magnification factor was $M = 0.19$. 5000 image-pairs were acquired at 50 Hz providing an observation-time of 100 s (corresponding to 40,000 D/U_∞). A stereoscopic imaging mapping function based on a camera pinhole model[14] was used for the calibration of the images. The first estimate of the mapping coefficients was obtained with a two-layer calibration plate (LaVision type 10) with equally spaced dots aligned with the laser sheet. A self-calibration procedure based on the disparity between images from left and right view[15]

was used to correct for residual misalignments between plate and laser sheet. Illumination and recording systems were synchronized with a LaVision *High Speed Controller* hosted by a PC using *Davis 8.3* software.

Intensity normalization was applied to the PIV recordings to reduce background intensity and light reflections from the model base. The residual background intensity was further attenuated subtracting the minimum intensity of a temporally sliding kernel of 11 images. An iterative multi-grid cross-correlation analysis based on window deformation[16] was used in the vector calculation with a 24 x 24 pixels (2.5 x 2.5 mm^2) final interrogation window and 75% overlap resulting in a 0.6 mm vector pitch. Spurious vectors were removed by means of the universal median filter[17].

The mean signal-to-noise ratio of the cross-correlation map, evaluated from 100 images, was approximately 4 in the separated region. The uncertainty was estimated to be approximately 2% of the free stream value[18] on the instantaneous velocity and 0.6% and 0.4% for the mean velocity and the RMS of the fluctuations respectively, based on the maximum RMS of the velocity fluctuations and the data ensemble size.[19]

3. Mean and instantaneous flow field

The time-average velocity field shown in Fig. 3 shows a progressive displacement of the backflow region with respect to the body center line with increasing misalignment, reaching a maximum value of 0.15 *D* at the largest investigated pitch angle of 1°.

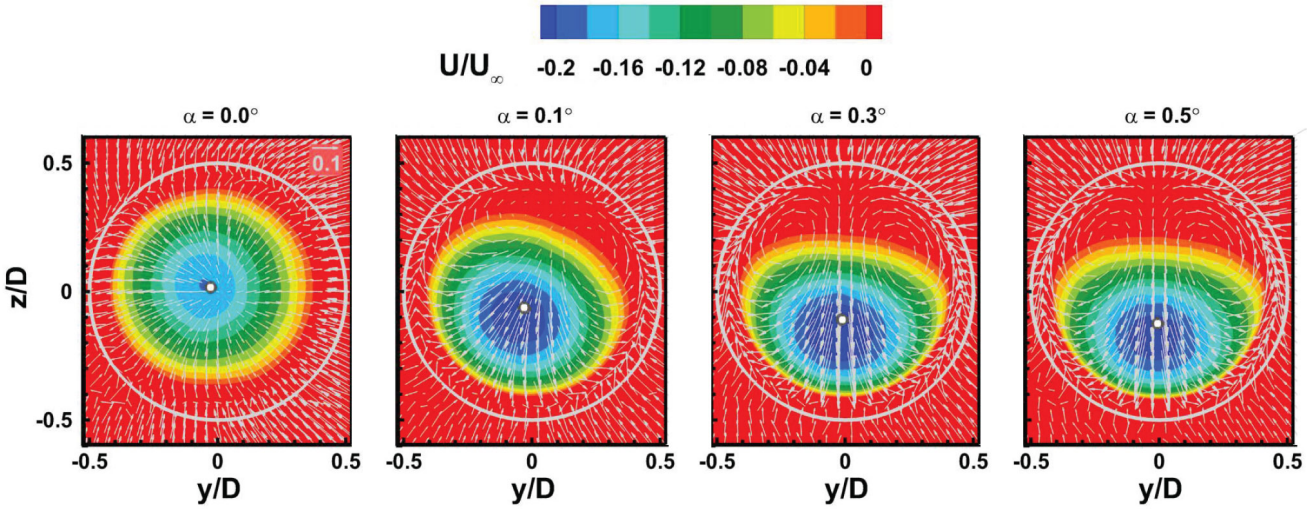

Fig. 2 Color contours of mean out-of-plane velocity *U*. Vectors plotted every 5th grid-point indicate in-plane components *V* and *W*. Mean backflow centroid indicated by white dot. Model base edge in solid gray. Observation-time is 40,000 D/U_∞.

This displacement is accompanied by a reduction of the fluctuations about the mean

position, as can be inferred from the root mean square (r.m.s.) of the backflow centroid relative displacement (see Fig. 3). A concurrent transformation of the mean in-plane flow topology can be appreciated, which changes from a source-like pattern, reflecting an approximately axisymmetric flow pattern that can be explained from an azimuthal meandering of the backflow region with no preferred orientation, to an in-plane counter-rotating recirculation pattern, which suggest the emergence of a preferred orientation of the wake[5].

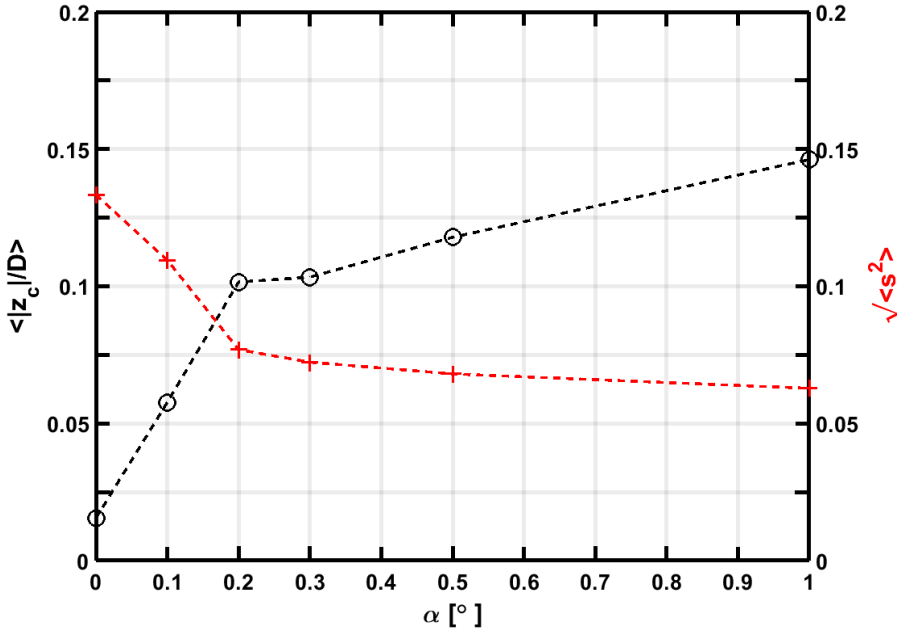

Fig. 3 Backflow centroid mean vertical position and r.m.s. of the relative displacement $\mathbf{s} = [(z_c(t) - \langle z_c \rangle)^2 + (y_c(t) - \langle y_c \rangle)^2]^{1/2}/D$ as a function of the pitch angle. Data averaged over 40,000 D/U_∞.

This behavior is illustrated in more detail in Fig. 4, where the trace of the backflow centroid position over the available observation-time is seen to evolve from a donut-like distribution, typically associated with azimuthal meandering, to a comparatively narrower elongated cloud as a result of the progressive confinement of the backflow centroid motion to its mean off-center position. This transition is reflected in the probability distributions of the relative backflow displacement, which displays a maximum at $s = 0.12$ and $s = 0.06$ for pitch angles of 0° and 0.1° respectively, while being monotonically decreasing for larger angles (Fig. 5 left), and furthermore in the azimuthal probability distributions which tend to narrow about a mean azimuthal orientation of $3\pi/2$ (Fig. 5 right).

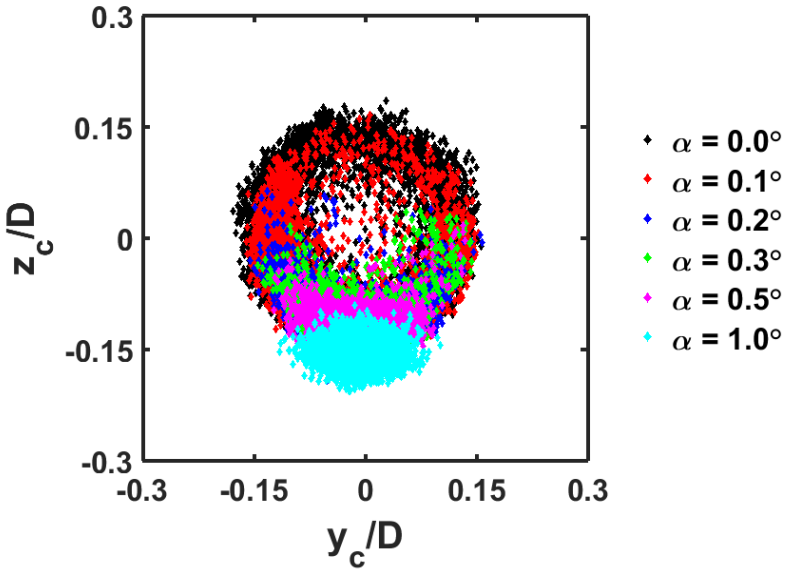

Fig. 4 Scatter-plot of the backflow centroid in-plane position over 40,000 D/U_∞.

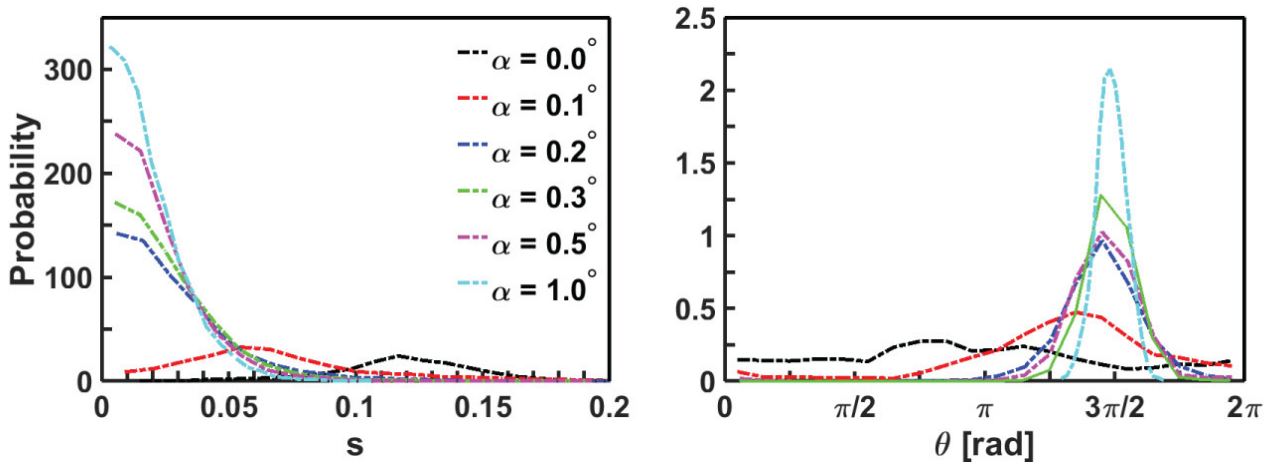

Fig. 5 Probability distributions of the relative displacement (left) and azimuthal position (right) of the backflow centroid.

Both the amplitude and the time scales of the backflow centroid motion tend to be reduced with increasing misalignment between the body and the incoming flow as can be inferred from Fig. 6. More specifically, the time history of the azimuthal coordinate reflects the transition from quasi-periodic fluctuations corresponding to a gradual precession about the model symmetry axis[4,5] to lower-amplitude and higher-frequency fluctuations about the long-time-average off-center position $\theta = 3\pi/2$.

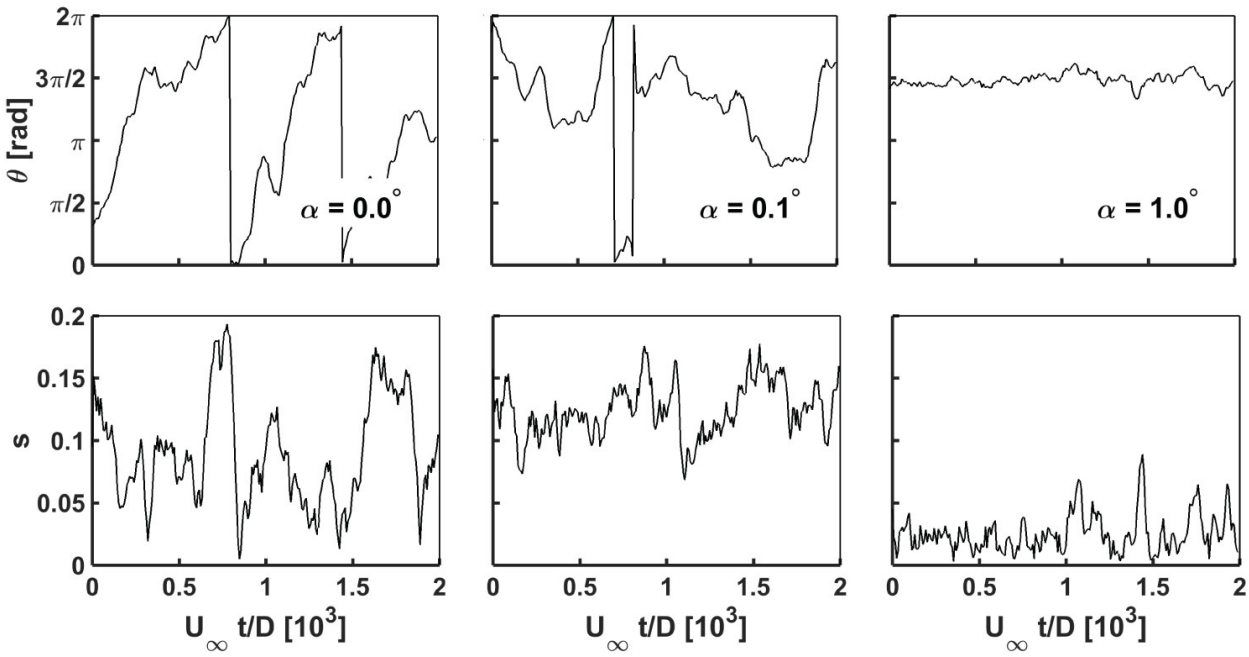

Fig. 6 Time-history of the backflow centroid position for increasing pitch angles. Azimuthal position (top) and relative displacement (bottom).

4. Proper Orthogonal Decomposition

Snapshot Proper Orthogonal Decomposition[13] was applied to the velocity fluctuations to investigate how the pitch angle affects the large-scale fluctuations occurring in the near-wake.

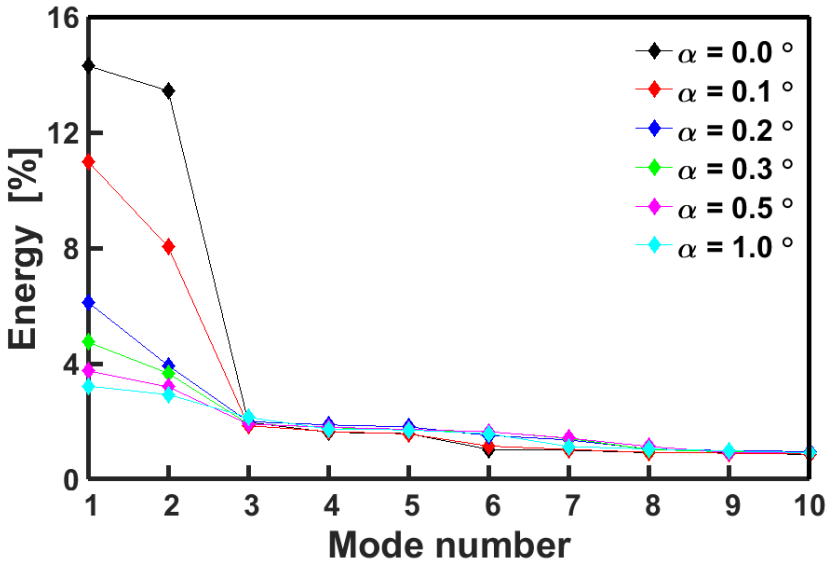

Fig. 6 Relative energy contribution of the first 10 POD modes.

The mode energy distributions in Fig. 6 show that the relative contribution of POD modes

$k = 1, 2$ reduces by approximately 80% when introducing a pitch angle in the order of 1°. The comparable strength and dipolar spatial arrangement (Fig. 7) of the associated spatial modes for the zero-pitch case is typically identified with the backflow meandering with no preference on the azimuthal orientation. It is observed that this pattern is increasingly distorted and tends to lose spatial coherence for misalignment angles of 0.3° or higher, while the two modes display qualitative differences, which fact can be linked with the emergence of a preferred azimuthal orientation of the shedding plane.

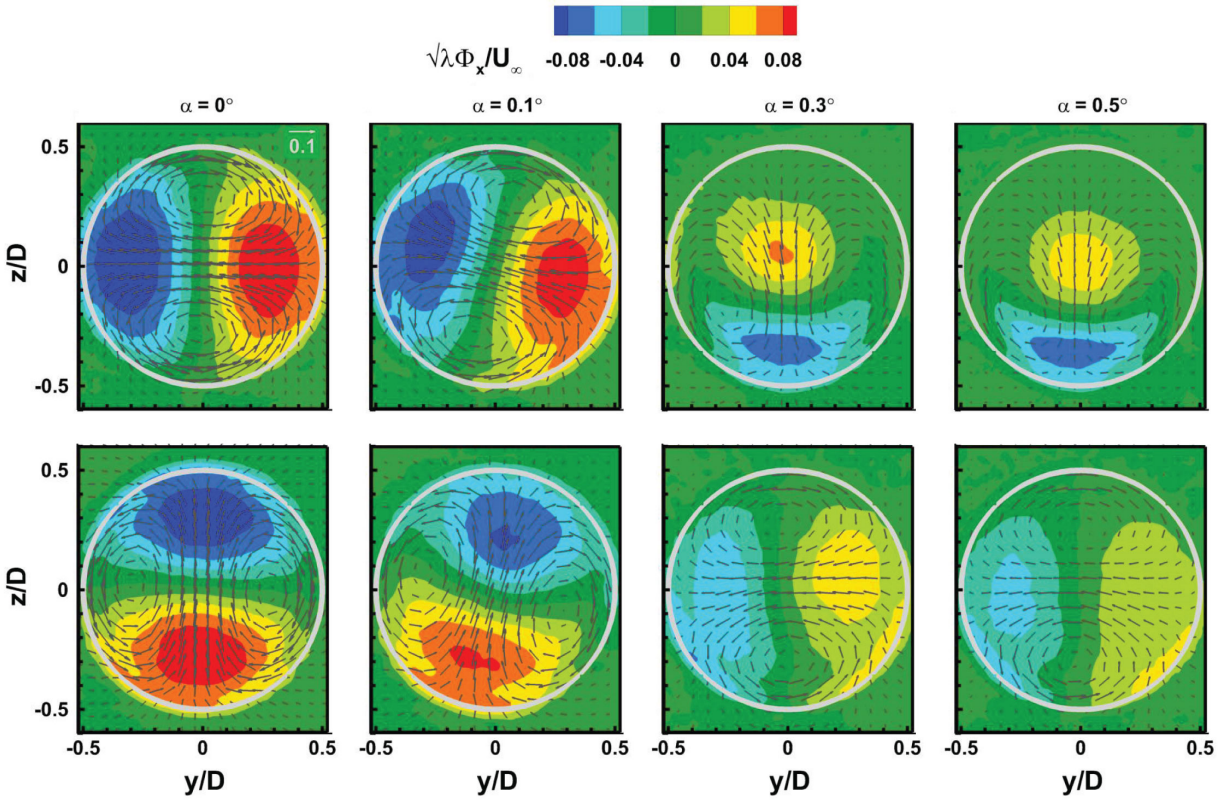

Fig. 7 Color contours of out-of-plane component of POD modes $k = 1$ (top) and $k = 2$ (bottom).

Finally the progressive inhibition of the long-term backflow instability is inspected from the frequency spectra of the first two POD mode time coefficients (Fig. 8). Significant contributions at the very-low frequency range corresponding to $St_D \sim 10^{-3}$ is only revealed under angular misalignments within 0.1°, whereas for larger angles the dominant contribution shifts towards a slightly higher frequency of $St_D = 0.002$ and can be only attributed to mode $k = 1$.

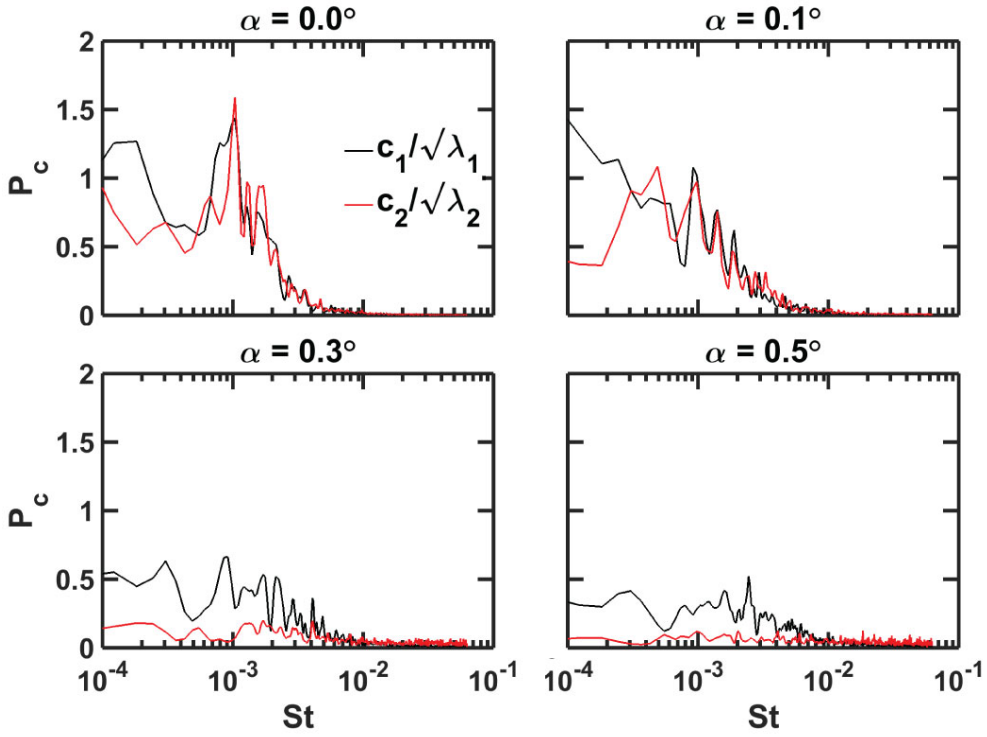

Fig. 8 Frequency spectra of POD time coefficients ; black: c1(t) and red: c2(t). Sampling frequency is 50 Hz. Strouhal number defined as $St_D = fD/U_\infty$.

5. Conclusions

The large-scale backflow instability in the near-wake of an blunt-based cylinder in pitch was investigated at $Re_D = 6.7 \cdot 10^4$, based on the model diameter. Time-resolved stereoscopic PIV measurements were conducted for pitch angles between 0° and 1° in a plane perpendicular to the free stream flow located $0.3\,D$ downstream of the model trailing edge. Long-time-average velocity fields show a radial offset of the reverse flow region from the model center-line increasing up to $0.15\,D$ with the pitch angle and a concurrent weakening of the fluctuations about the mean position. Analysis of the time history of the backflow centroid position further reveals a gradual reduction of the fluctuations, which is associated to the transition from large-scale backflow meandering to a progressive locking to the mean off-center position.

The relative contribution of the first two velocity POD modes $k = 1$ and $k = 2$ reduces by about 80% when increasing the pitch angle up to 1°, while their dipolar spatial distribution typical of backflow azimuthal meandering was found to become distorted already under misalignments from 0.3° or above, in line with the emergence of a preferred azimuthal orientation of the shedding plane under asymmetric inflow conditions. The frequency

spectra of the corresponding POD mode time coefficients display a contribution at $St_D \sim 10^{-3}$ only under deviations within 0.1° from axisymmetric inflow conditions, which further endorses the hypothesis of the strong inhibitive effect of misalignment on the azimuthal backflow meandering.

7. References

[1] Chomaz, J.M. (2004) Global instabilities in spatially developing flows: Non - normality and nonlinearity. Ann Rev Fluid Mech 2(37):357 - 92. doi:10.1146/annurev.fluid.37.061903.175810.

[2] Fuchs, H.V., Mercker, E., and Michel, U. (1979) Large-scale coherent structures in the wake of axisymmetric bodies. J Fluid Mech 93:185 - 207. doi:10.1017/S0022112079001841.

[3] Achenbach, E. (1974) Vortex shedding from spheres. J Fluid Mech 62:209 - 221. doi:10.1017/S0022112074000644.

[4] Rigas, G., Oxlade, A.R., Morgans, A.S., and Morrison, J. (2014) Low - dimensional dynamics of a turbulent axisymmetric wake. J Fluid Mech 755:R5.

[5] Grandemange, M., Gohlke, M., and Cadot, O. (2014). Statistical axisymmetry of the turbulent sphere wake. Exp Fluids 55:1838. doi: 10.1007/s00348 - 014 - 1838 - x.

[6] Gentile, V., Schrijer, F.F.J., van Oudheusden, B.W., Scarano, F. (2015) Time - dependent behaviour of the recirculation region behind an axisymmetric bluff - body. Proceedings of the 9th Symposium on Turbulence and Shear Flow Phenomena TSFP - 9.

[7] Fabre, D., Auguste, F., Magnaudet, J. (2008) Bifurcations and symmetry breaking in the wake of axisymmetric bodies. Ph Fluids 20:051702. doi:10.1063/1.2909609.

[8] Wolf, C.C, You, Y., Hörnschemeyer, R., Lüdeke, H., Hannemann, V. (2013) Base - flow sensitivity of a generic rocket forebody towards small freestream angles. Progress in Flight Physics 5:155 - 168. doi: 10.1051/eucass/201305169.

[9] Grandemange, M., Gohlke, M., Parezanović, V., and Cadot, O. (2012). On experimental sensitivity analysis of the turbulent wake from an axisymmetric blunt trailing edge. Ph Fluids 24:035106. doi: 10.1063/1.3694765.

[10] Ashok, A. Van Buren, T., and Smits, A.J. (2015). Asymmetries in the wake of a submarine model in pitch. J Fluid Mech 774:416 - 442. doi:10.1017/jfm.2015.277.

[11] Ashok, A. Van Buren, T., and Smits, A.J. (2015). The structure of the wake generated by a submarine model in yaw. Exp Fluids 56:123. doi:10.1007/s00348 - 015 - 1997 - 4.

[12] Oxlade, A.R., Morrison, J.F., Qubain, A., and Rigas, G. (2015). High - frequency forcing of a turbulent axisymmetric wake. J Fluid Mech 770:305 - 318. doi:10.1017/jfm.2015.153

[13] Sirovich, L. (1987) Turbulence and the dynamics of coherent structures. Part 1 - 3", Quarterly of Applied Mathematics XLV 3:561 - 590.

[14]Soloff, S. M., Adrian, R. J., and Liu, Z. C. (1997) Distortion compensation for generalized stereoscopic particle image velocimetry. Meas Sci Technol 8(12):1441 - 1454.

[15]Wieneke, B. (2005) Stereo - PIV using self-calibration on particle images. Exp Fluids 39(2):267 - 280.

[16]Scarano, F., and Riethmuller, M.L. (2000) Advances in Iterative Multigrid PIV Image Processing. Exp Fluids 29(1):51 - 60.

[17]Westerweel, J., and Scarano, F. (2005) Universal Outlier Detection for PIV Data. Exp Fluids 39(6):1096 - 1100.

[18]Raffel, M., Willert, C. E., Wereley, S., and Kompenhans, J. (1996) Particle Image Velocimetry: A Practical Guide. 2nd ed., Springer - Verlag Berlin Heidelberg.

[19]Benedict, L. H., and Gould, L. D. (1996) Towards better uncertainty estimates for turbulence statistics. Exp Fluids 22(2):129 - 136.